

Observation of a quasi-1D Mott-Hubbard insulator: The re-entrant Na/Si(111)- 3×1 surface

J. R. AHN¹, N. D. KIM¹, S. S. LEE¹, K. D. LEE¹, B. D. YU²,
D. JEON³, K. KONG⁴ and J. W. CHUNG¹

¹ *Physics Department and Basic Science Research Institute, Pohang University of Science and Technology - San 31 Hyoja Dong, Pohang 790-784, Korea*

² *Department of Physics, University of Seoul - 90 Cheonnong-dong Tongdaemun-gu, Seoul 130-743, Korea*

³ *Department of Physics, Myong Ji University - Yongin Kyunggi-Do Seoul 449-728, Korea*

⁴ *IQUIPS, University of Seoul - 90 Cheonnong-dong, Tongdaemun-gu Seoul 130-743, Korea*

(received 13 August 2001; accepted 19 December 2001)

PACS. 71.30.+h – Metal-insulator transitions and other electronic transitions.

PACS. 73.20.-r – Electron states at surfaces and interfaces.

PACS. 61.18.-j – Other methods of structure determination.

Abstract. – We have investigated the origin of a semiconducting phase of the re-entrant Na/Si(111)- 3×1 surface formed by adding extra adatoms on the earlier 3×1 phase at $1/3$ monolayers (MLs). The additional Na adatoms are found to form quasi-one-dimensional (1D) atomic chains in our scanning tunnelling microscopy images while keeping the surface semiconducting. The unique features in our valence band and in high-resolution electron-energy-loss spectra suggest that the re-entrant 3×1 surface is a Mott-Hubbard-type insulator. We thus report a novel quasi-1D insulator-insulator transition where electron-electron correlation plays a decisive role.

Despite the remarkable success of a single-electron band theory to understand electrical properties of solids, the theory often fails to explain some notable properties of solids where electron-electron correlation (EEC) plays a significant role [1]. Recently, several such examples have been reported especially for two-dimensional (2D) correlated electron systems where metallic surfaces become various forms of insulators [2–8]. This occurs mainly as a result of subtle interplay between the intrasite Coulomb repulsion U and other interactions such as the nearest-neighbor intersite hopping energy t , disorder in the form of random site potential, and the electron-phonon interaction. A Mott-Hubbard insulator, in particular, is found when U dominates over t in a frozen lattice, and is typically manifested by the appearance of two new valence bands, *i.e.*, one filled band and another one empty separated by U . These bands are split off from a metallic band at the Fermi energy. Here we report a case where EEC drives a quasi-1D (Q-1D) band-insulator into a Q-1D Mott-Hubbard insulator, which has never been

observed before. The system is a re-entrant Na/Si(111)- 3×1 surface (3×1 -II for brevity) at the Na coverage $\theta = 2/3$ monolayers (MLs). It is formed by adding extra Na atoms onto the earlier 3×1 surface at $1/3$ ML (3×1 -I hereafter) while maintaining the surface semiconducting. Although an active role of EEC has been suggested previously since the 3×1 -II surface is predicted to be metallic by a single-electron band picture, no clear evidence of it has been presented [9].

We here discuss experimental evidence of the driving mechanism for the Q-1D Mott-Hubbard insulating state of the 3×1 -II surface, which is well supported by our calculation based on a density functional theory including EEC. The structural and electronic properties of the surface have been obtained by using three diagnostic tools including high-resolution electron-energy-loss spectroscopy (HREELS), scanning tunnelling microscopy (STM), and photoelectron spectroscopy (PES) using synchrotron photons. All measurements have been made in three separate UHV chambers: a Leybold-Heraeus ELS-22 spectrometer with an optimum resolution of 3 meV and a half-acceptance angle of 2° , an STM chamber equipped with a low-energy electron diffraction (LEED), and an angle-resolved PES chamber using photons of energy 21.2 eV with energy resolution of 140 meV. The base pressure of all the three chambers was in the range of low 10^{-11} Torr. The sample was cut from a boron-doped Si(111) wafer ($\rho \sim 1.5 \Omega\text{cm}$), and cleaned by a well-known recipe [9]. The Na coverage was monitored by measuring the work function change ($\Delta\phi$) from the shift of the secondary electron tail in X-ray photoemission spectra [9, 10]. For comparison, all our measurements were made by increasing θ from the 3×1 -I surface at $\Delta\phi = -0.9$ eV. For brevity, we denote Na_I and Na_{II} for the Na atoms on the 3×1 -I surface and the additional Na atoms on the 3×1 -II surface, respectively.

We first discuss the evolution of the atomic arrangement as a function of θ ($\leq 2/3$ ML) revealed in our STM images presented in fig. 1. A filled-state STM image of the 3×1 -I surface at $1/3$ ML in fig. 1(a) shows the well-known Q-1D zig-zag Si honeycomb chains with Na_I atoms at the channel sites between the chains [8]. The rather fuzzy nature of our STM images turns out to be the intrinsic property of the Na-added surface in addition to thermal fluctuation at room temperature. Extra Na adatoms (Na_{II}) added on this 3×1 -I surface, which appear as bright spots in fig. 1(b), are seen to occupy the sites between the Na_I chains. With further increase in θ , these Na_{II} adatoms tend to form atomic chains in parallel to the Na_I chains and eventually form a well-ordered 3×1 -II surface at $2/3$ ML as shown in fig. 1(c). As discussed later, this surface turns out to be semiconducting with origin different from that of the 3×1 -I surface. We attempt to exploit how EEC can drive a Q-1D band-insulating 3×1 -I surface into another form of insulator for the Q-1D 3×1 -II surface in this peculiar Q-1D insulator-insulator transition. In order to quantify our experimental observations, we have performed first-principles total-energy calculations using density functional theory (DFT). Total energies and forces were calculated within the local density approximation (LDA) for the exchange-correlation functional using pseudopotentials and a plane-wave basis with a cutoff energy of 10 Ry, as implemented in the FHI96MD code [11].

The atomic arrangement of the 3×1 -I surface at $1/3$ ML has been well documented both theoretically [12, 13] and experimentally [14, 15], known as a missing-Pandey-chain (MPC) model. Our calculations also confirm the MPC as the most stable structure at $1/3$ ML (fig. 2(a)). This occurs by the charge transfer from Si atom 5 and Na_I to the Si edge atoms 1 and 4, and the formation of a double bond between the Si atoms 2 and 3. Simulation shows that the zig-zag chains in the STM images are produced by filled states of the Si atoms 1 and 4, while the dark lines are from empty states of the Si atoms 2 and 3 [12]. The bright spots from the Na_{II} atoms on the dark lines in fig. 1(b) explicitly show the binding sites of the Na_{II} atoms somewhere between the Si atoms 2 and 3. In fact, our calculated 3×1 -II surface

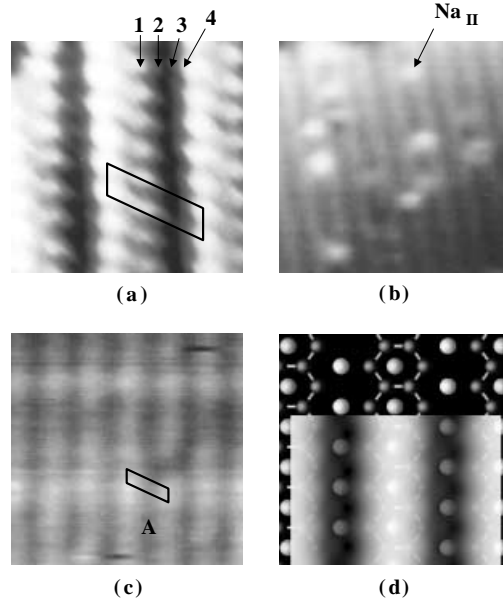


Fig. 1 – Changes in the STM images by Na_{II} adatoms. (a) A well-defined 3×1 -I at $1/3$ ML exhibiting the zig-zag Si honeycomb chains. The numbers are explained in fig. 2. (b) A small number of Na_{II} atoms ($V_s = -1.6$ V) added on the 3×1 -I surface appear as bright spots on the dark lines. (c) With further dose of Na_{II} , a well-ordered 3×1 -II surface is eventually formed at $2/3$ ML ($V_s = -1.6$ V), where the Na_{II} chains appear as the bright straight lines. Notice the dimmed bright straight lines in contrast to the zig-zag chains at $1/3$ ML. (d) A simulated filled-state STM image ($V_s = -1.5$ V) of the buckled MPC model (fig. 2(b)) shown in the background reproduces the image in (c). The tilted rectangles in (a) and (c) denote a 3×1 unit cell.

(fig. 2(b)) reveals that the Na_{II} atoms occupy the hollow sites slightly off-centered inside the Si honeycombs. The extra Na_{II} atoms are found to induce quite a large buckling (~ 0.71 Å) of the top-layer Si dimer atoms 2 and 3 (see the side view) in sharp contrast to the symmetric and planar Si surface layer at $1/3$ ML. The calculated STM image of the 3×1 -II surface shown in fig. 1(d) with the atomic structure in the background reproduces quite well the somewhat fuzzy nature of the image in fig. 1(c) mainly due to the rather broad charge distribution along the Si honeycomb chains. Before the completion of the 3×1 -II surface, a distribution of the 6×1 surface and the 3×2 surface has been observed also in our STM images (not shown) as reported earlier [9]. From fig. 1(a) and (c), we confirm the Na coverages of the 3×1 -I and 3×1 -II surfaces as $1/3$ ML and $2/3$ ML, respectively. Similarly we obtain $1/2$ ML for the 6×1 surface.

Having characterized the atomic arrangements, we now examine the electrical property of the surface. The semiconducting nature of the 3×1 -I surface with a band gap of about 1.2 eV is well understood in terms of the MPC model without resorting to the EEC. The 3×1 -I surface is thus believed to be a simple band-insulator. Figure 3 shows the spectral evolutions with increasing θ for the valence band PES (left) and the HREELS (right) data. The spectral features S_1 , S_2 , and S_3 in the valence band of the 3×1 -I surface are the three different bonding states resulting from the Na-Si hybridization [12, 13]. The loss peak SL_1 at 1.8 eV is attributed to an interband transition from the S_1 π -bonding state to a π^* -antibonding state. Notice that the 3×1 -II surface at $2/3$ ML (top spectra) appears to be semiconducting as seen

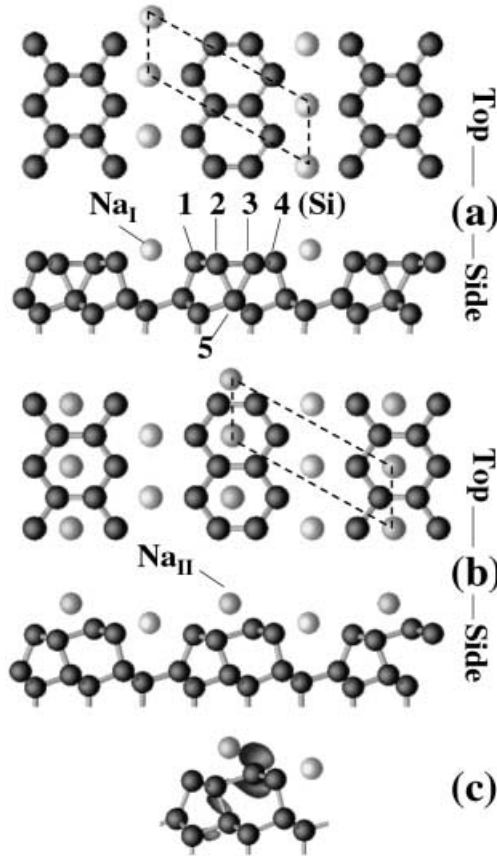


Fig. 2 – Fully relaxed atomic structures of the MPC models for Na/Si(111)- 3×1 surfaces: (a) the 3×1 -I at $1/3$ ML and (b) the 3×1 -II at $2/3$ ML. The tilted rectangles are the unit cells. Note that the Na_{II} atoms occupy the slightly off-centered hollow sites in the Si honeycombs. We find that the electron of Na_{II} , instead of Si atom 5, is transferred to the Si edge atoms to form a polarized lone-pair orbital. As a result, the π -bonded symmetric Si dimer becomes unstable and the Si atoms 2 and 5 form a sp^3 -like bond causing the buckling of the top Si layer. As shown in (c), this buckling generates a non-bonding orbital at the Si atom 3, leading to a half-filled dangling bond. Despite the half-filled dangling bonds predicted here, the 3×1 -II surface is found to be semiconducting, suggesting a critical role of EEC in driving the surface semiconducting.

by the absence of density of states near the Fermi energy in the PES and by the finite band gap (0.8 eV) determined by the loss energy of the new loss peak SL_2 in the HREELS spectra.

In contrast to this observation, our LDA calculation in fig. 4 predicts the 3×1 -II surface metallic as indicated by a flat band (the LDA dotted curve) that crosses the Fermi energy ($E_F = 0$). This flat band (band width $W \leq 0.2$ eV) is found to stem from the dangling bonds of the Si atom 3. Since there is one unsaturated dangling bond per 3×1 unit cell, the dangling-bond band is half-filled. This metallic band, however, has never been observed experimentally. Instead, one clearly finds a new state (marked as S_4 in fig. 3), which appears at the onset of the 3×1 -II surface (~ 0.58 ML) and becomes most prominent at the completion of the 3×1 -II surface. Although not shown here, the S_4 is found to form a flat band extending over 0.67 \AA^{-1} along the $\bar{\Gamma}$ - \bar{C} azimuth, perpendicular to the chain direction, exhibiting its Q-1D

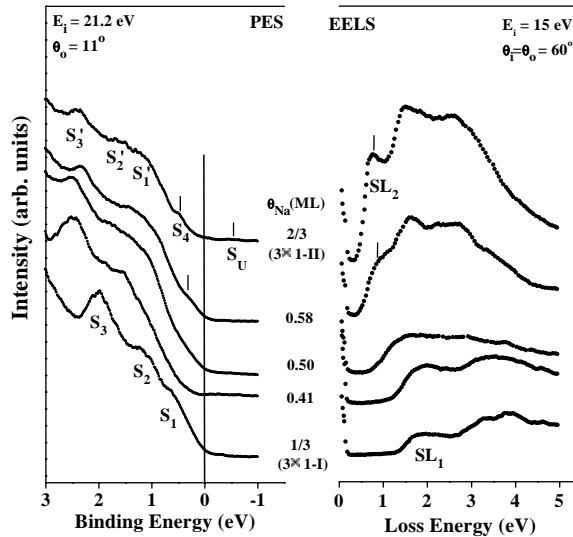


Fig. 3 – Spectral evolution of the valence band photoemission (left) and HREEL spectra (right) as Na_{111} atoms adsorb on the 3×1 -I surface. Notice that a new surface state (S_4) appearing at the onset of the 3×1 -II surface in PES accompanies a unique loss peak (SL_2) in HREELS. As discussed in the text, the SL_2 stems from interband transition between the S_4 and the empty state S_U . The PES data were obtained with the emission angle at 11° where spectral changes near E_F are most pronounced.

nature. Paggel *et al.* also noted the presence of the S_4 state previously [16]. Since the substrate structure has not been changed significantly with θ up to $2/3$ ML, the EEC interactions are expected to play a vital role in keeping the surface semiconducting. We therefore calculated the surface bands in the LDA including the intrasite Coulomb repulsion U . The calculation employs a single-band Hubbard model [17] for the half-filled surface state in which the U of the Si dangling bond is explicitly taken into account.

We determined the parameter U by performing LDA calculations for the various possible charge states of the Si dangling bond: It holds $U = E(+) + E(-) - 2E(0)$, where $E(+)$, $E(-)$, and $E(0)$ represent the ground-state energies of a positively charged, a negatively charged, and a neutral state, respectively [4]. To simulate the one isolated Si dangling bond, an enlarged 3×2 surface unit cell was used in which the other Si dangling bond was saturated with a hydrogen atom. Our result shown in fig. 4 reveals that the flat metallic surface band near E_F becomes split into a completely filled lower Hubbard band (LHB) and an empty upper Hubbard band (UHB) with a Hubbard gap U . We obtain $U = 0.79$ eV corrected by the spin-polarization energy of -0.12 eV for the neutral dangling bond [18]. This value of U may be compared to the value of 0.9 eV obtained for the usual Si dangling bond on a Si(111) surface [18]. Therefore the 3×1 -II surface is predicted to be a Mott-Hubbard-type insulator by our calculation. The calculated U much greater than the intersite hopping energy $t (= W/2z (\leq 0.1$ eV), where z is the coordination number, 3 for the Si atoms 2 and 3) supports the prediction.

The prediction of a Mott-Hubbard insulator is fully consistent with our experimental observation in fig. 3 when we identify the S_4 band as the LHB and the SL_2 as the inter-Hubbard band transition [6]. The empty S_U band then forms the UHB of the 3×1 -II surface. We can then estimate U directly from the loss energy of the SL_2 peak. Other than interband transition, there are several possible sources that can produce a loss peak such as the SL_2 including a local Na-Si vibrational excitation, a surface plasmon, and a surface phonon.

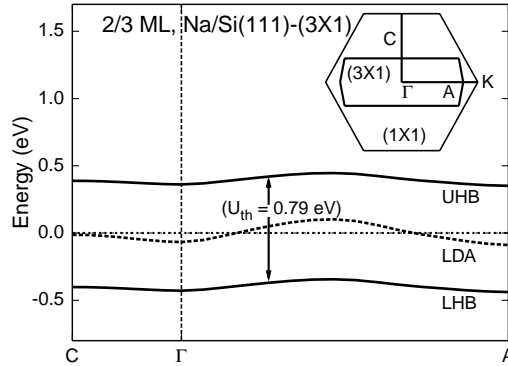


Fig. 4 – Band structure of the 3×1 -II surface calculated in LDA and LDA+ U . All energies are referenced to the Fermi energy. The dotted curve is a metallic band (not observed experimentally) calculated in LDA. In LDA+ U , this metallic band is found to split into a lower (LHB) and an upper Hubbard band (UHB) with a band gap $U = 0.79$ eV as seen in our spectra. The inset shows the 3×1 surface Brillouin zone (SBZ) inside the 1×1 SBZ.

All these sources, however, are not quite likely the case as discussed previously [6]. The significantly higher loss energy ($E_L \sim 0.8$ eV) and an order of magnitude broader linewidth of the SL_2 ($W_L \geq 0.1$ eV) compared to the corresponding values of a typical metal-Si vibrational mode ($E_L \leq 0.025$ eV, $W_L \leq 0.01$ eV) [19,20] easily rule out the vibrational origin. Also it is not hard to show that a several order of higher carrier concentration is required to excite a surface plasmon of a similar energy with that of the SL_2 . Finally, the absence of multi-phonon peaks in our spectra simply excludes the possibility of a single-phonon loss peak for the SL_2 . With the presence of the split Hubbard bands, the 3×1 -II surface could either be a Mott-Hubbard insulator or a bipolaronic insulator depending on the absence or presence of a local lattice distortion, respectively [9]. We, however, rule out the bipolaronic mechanism simply because it requires a 3×2 unit cell for the 3×1 -II semiconducting surface [3,5,21,22] in sharp contradiction with the dominating 3×1 unit cells observed in our STM images. Moreover, no 3×2 LEED pattern has been observed for all θ up to the saturation.

By identifying the S_4 band as the LHB and the SL_2 loss peak as the inter-Hubbard band transition, we obtain $U = 0.8$ eV. Therefore our measured binding energy of the LHB ($U/2 = 0.40 \pm 0.02$ eV) agrees almost perfectly with the predicted theoretical value [18]. As an alternative test for a Mott-Hubbard insulator, we examine if the experimental value of U satisfies a so-called Hubbard criterion $U > nW$ ($1.0 \leq n \leq 1.8$), where W is the band width of a Hubbard band [1]. As discussed earlier [6,23], we estimate W of the LHB from the linewidth W_L of the loss peak SL_2 using $W_L = \sqrt{W^2 + W_t^2}$ assuming that the band widths of LHB and UHB are equal. Here W_t is an instrumental transfer width. Using the experimental values $W_L \sim 0.200$ eV and $W_t \leq 0.035$ eV, we obtain $W \leq 0.197$ eV. We thus find that the ratio $U/W = 4.1$ (> 1.2) satisfies the criterion quite well as a Mott-Hubbard insulator. We thus conclude that *the semiconducting 3×1 -II surface at $2/3$ ML is a Q-1D Mott-Hubbard insulator.*

In summary, we report a Q-1D Mott-Hubbard semiconducting state observed on the re-entrant Na/Si(111)- 3×1 surface at $2/3$ ML. The Q-1D Mott-Hubbard semiconducting surface is manifested by a new surface state at 0.45 eV below the Fermi energy in the valence band identified as a lower Hubbard band. The interband transition between the split Hubbard bands appears as a unique loss peak in our HREELS spectra, which allows us to estimate both the

Hubbard repulsion energy $U = 0.8\text{ eV}$ and the intersite hopping energy $t \leq 0.1\text{ eV}$. These values are confirmed by our DFT calculations based on a single-band Hubbard model. The much greater U compared to t is thought to drive the 3×1 -II surface at $2/3$ ML semiconducting rather than metallic otherwise predicted by a single-electron band theory.

* * *

We acknowledge partial supports by the BSRI 99-2440, also by the POSTECH research fund under Grant No. 1RB9910701, and by the Korea Research Foundation Grant (KRF-99-015-DP0134). BDY also acknowledge support from the Korea Science and Engineering Foundation through the ASSRC at Yonsei University.

REFERENCES

- [1] For example, see MOTT N. F., *Metal-Insulator Transitions*, 2nd edition (Taylor and Francis, New York) 1990.
- [2] CARPINELLI J. M. *et al.*, *Nature*, **381** (1996) 398.
- [3] PANKRATOV O. and SCHEFFLER M., *Phys. Rev. Lett.*, **71** (1993) 2797.
- [4] NORTHRUP J. E. and NEUGEBAUER J., *Phys. Rev. B*, **57** (1998) R4230.
- [5] WEITERING H. H. *et al.*, *Phys. Rev. Lett.*, **78** (1997) 1331.
- [6] AHN J. R. *et al.*, *Phys. Rev. Lett.*, **84** (2000) 1748.
- [7] DINARDO N. J., MAEDA T. and PLUMMER E. W., *Phys. Rev. Lett.*, **65** (1990) 2177.
- [8] JEON D. *et al.*, *Phys. Rev. Lett.*, **69** (1992) 1419.
- [9] LEE K. D. and CHUNG J. W., *Phys. Rev. B*, **57** (1998) R2034.
- [10] WEITERING H. H. *et al.*, *Phys. Rev. B*, **49** (1994) 16837.
- [11] BOCKSTEDTE M. *et al.*, *Comput. Phys. Commun.*, **107** (1997) 187.
- [12] KANG M. H. *et al.*, *Phys. Rev. B*, **58** (1998) R13359.
- [13] ERWIN S. C. and WEITERING H. H., *Phys. Rev. Lett.*, **81** (1998) 2296.
- [14] CALLAZO-DAVILA C. *et al.*, *Phys. Rev. Lett.*, **80** (1998) 1678.
- [15] LOTTERMOSER L. *et al.*, *Phys. Rev. Lett.*, **80** (1998) 3980.
- [16] PAGGEL J. J. *et al.*, *Surf. Sci.*, **414** (1998) 221.
- [17] HUBBARD J., *Proc. R. Soc. London, Ser. A*, **281** (1964) 401.
- [18] NORTHRUP J. E., *Phys. Rev. B*, **40** (1989) 5875.
- [19] CLOTET A. *et al.*, *Phys. Rev. B*, **51** (1995) 1581.
- [20] IBACH H. and MILLS D. L., *Electron Energy Loss Spectroscopy and Surface Vibrations* (Academic Press, New York) 1982.
- [21] KUBO O. *et al.*, *Surf. Sci. Lett.*, **415** (1998) L971.
- [22] PLUMMER E. W. and DOWEN P. A., *Prog. Surf. Sci. V*, **42** (1993) 201.
- [23] LAITENBURGER P. and PALMER R. E., *Phys. Rev. Lett.*, **76** (1996) 1952.